Model With Distributed Vectorial Premotor Bursters Accounts for the Component Stretching of Oblique Saccades

CHRISTIAN QUAIA AND LANCE M. OPTICAN
Laboratory of Sensorimotor Research, National Eye Institute, Bethesda, Maryland 20892

Quaia, Christian and Lance M. Optican. Model with distributed vectorial premotor bursters accounts for the component stretching of oblique saccades. *J. Neurophysiol.* 78: 1120–1134, 1997. During oblique saccades, the durations of the horizontal and vertical components are stretched until they are approximately equal. Models of the saccadic system have been proposed that provide a mechanism for that stretching. However, they fail to simulate the pattern of activity recorded from premotor medium lead burst neurons (MLBNs) in the brain stem. A new model of the saccadic system is proposed that accounts for both the component stretching of oblique movements and the pattern of activity recorded in MLBNs. MLBNs that project to horizontal (or vertical) motoneurons actually have a wide span of on-directions (the direction associated with the largest discharge) around the cardinal direction. We infer from the wide span of their on-directions that, at the level of individual MLBNs, the vectorial signal present in spatially organized structures (e.g., the superior colliculus) is not decomposed into the separate horizontal and vertical components represented by the motoneurons. Nonetheless, all prior models of the saccadic system have decomposed the vectorial premotor command into horizontal and vertical commands at the level of the MLBNs. That decomposition was *explicit*, because individual MLBNs, with a sine- or cosine-shaped directional tuning curve, were used. We propose here that the decomposition into horizontal and vertical commands is carried out only at the level of the motoneurons. This decomposition is *implicit*, because no single MLBN encodes the horizontal or vertical command; the command only exists implicitly in the activity of the population of MLBNs. The new vectorial burster model correctly simulates the pattern of activity recorded in primate MLBNs, and the components of its oblique saccades are stretched. Two mechanisms contribute to this stretching: the distribution of MLBN tuning curves and the inhibition exerted by the contralateral population of MLBNs. In contrast, feedback control of the saccade contributes negligibly to the stretching. Even though the vectorial burster model predicts a component stretching, it is not constrained to produce perfectly straight oblique saccades because no trajectory control is implemented. The amount of curvature depends on the similarity of the horizontal and vertical systems (both neural and mechanical). In this model, stretching is interpreted simply as a side effect of the properties of the MLBNs' tuning curves. The distributed MLBNs of the vectorial burster model forces the general organization of the saccadic system to be reconsidered. We propose that a distributed architecture in which several different neural systems cooperate is needed.

INTRODUCTION

Saccades are the fast eye movements that we use to redirect our gaze from one point of interest to another. Eye movements are controlled by three pairs of muscles; the pairs that control horizontal and vertical movements lie in almost horizontal and saggital planes, respectively (Robinson 1982). However, the commands for evoking saccades are generated by premotor structures, like the superior colliculus, that are organized vectorially (Robinson 1972; Schiller and Koerner 1971; Schiller and Stryker 1972; Sparks and Mays 1990; Wurtz and Goldberg 1971, 1972). Thus vectorial neural commands to make oblique saccades must be decomposed to obtain the correct horizontal and vertical motor commands. Prior models of the saccadic system used an *explicit* decomposition of the vectorial commands into horizontal and vertical commands on premotor burst neurons. In this paper, we propose a novel vectorial model that performs this decomposition without computing separate horizontal and vertical commands at the level of individual neurons. Instead, the decomposition into separate horizontal and vertical commands does not occur until the level of the motoneurons.

Models of horizontal saccades

Early studies of saccades were simplified by concentrating on horizontal movements. These studies led to the development of what is considered a milestone in the modeling of the saccadic system, the Robinson model (Robinson 1975; Zee et al. 1976). This model, taking into account anatomic and physiological data, proposed the notion that horizontal saccades are produced by a pulse-step signal applied to the motoneurons. In that model, and in all the models derived from it, the pulse is shaped by a local feedback loop that continuously feeds a burst generator with an estimate of the current motor error. The step of innervation then is obtained by integrating the pulse. This model succeeded in generating realistic horizontal saccades, showing the well-known relationships among amplitude, duration, and peak velocity (the so-called *main sequence*), characteristic of experimentally recorded saccades (Bahill et al. 1975; Baloh et al. 1975). Of particular relevance to this study is that the duration of a saccade increases with its amplitude.

Studies of oblique saccades

However, most saccades are neither horizontal nor vertical, but oblique. For this reason, beginning in the late 1970s, more and more studies on saccades dealt with oblique movements (Bahill and Stark 1977; Evinger et al. 1981; Guitton and Mandl 1980; King et al. 1986; Viviani et al. 1977). The simplest possible model (Bahill and Stark 1975; Bahill and Stark 1977; Tweed and Vilis 1985; Van Gisbergen et al. 1985) for describing oblique movements was obtained simply by adding, in parallel to the model of the horizontal saccadic system, a vertical pulse generator. This vertical

system was controlled by a second local feedback loop generating a signal proportional to the vertical motor error. This scheme is generally known as the independent model (Fig. 1*A*). Such an arrangement would lead to fast, but curved, saccades because the large component would have a longer duration than the small component. However, experimental observations revealed that the saccades generated by the independent model differ from those recorded in either humans, monkeys (cf. Fig. 2), or cats. In particular, the duration of the smaller component is stretched (Becker and Jürgens 1990; Evinger and Fuchs 1978; Guitton and Mandl 1980; King et al. 1986; Smit et al. 1990; Van Gisbergen et al. 1985), so that oblique trajectories tend to be straighter than predicted by the independent model. Another important aspect of oblique saccades is their large intersubject and interspecies variability, i.e., one subject can make straighter saccades than another. Furthermore, there is also an intrasubject variability, i.e., the same subject can make differently curved saccades in the same experimental session (Becker and Jürgens 1990; Viviani et al. 1977).

Early models of oblique saccades

To account for the stretching of the smaller component of oblique saccades, several different models have been developed. We can group these models into two categories: the common source models and the cross-coupled models. The first category is represented by the model developed by Van Gisbergen and colleagues (Van Gisbergen et al. 1985) and its derivations (Fig. 1*B*). In these models, rather than two independent pulse generators, there is a single, vectorial, pulse generator. The input to this element is the current vectorial motor error, and its output, the vectorial pulse, is decomposed into the horizontal and vertical components (by multiplication with the cosine and the sine of the angle of elevation of the saccade, respectively). This arrangement leads to perfectly straight saccades, which are as fast as cardinal (i.e., pure horizontal or pure vertical) saccades of the same amplitude, rather than the mildly curved saccades commonly observed. Another criticism of this model is that the duration of the two components is always the same, whereas studies (Bahill and Stark 1977; Becker and Jürgens 1990; King et al. 1986) have shown that the two components can terminate at slightly different times.

The second family of models (cross-coupled) is based on separate, but not independent, pulse generators (Fig. 1*C*). In the first of these models (Grossman and Robinson 1988), the output of one pulse generator exerts an inhibitory effect on the other, functionally reducing its gain (Fig. 1*C*, *arrow 2*). By varying the amount of this cross inhibition, it is possible to simulate saccades of different curvature and different velocity, but, as pointed out elsewhere (Becker and Jürgens 1990), it is not easy to obtain simultaneously both realistic trajectories and realistic velocity profiles. Another model has been proposed in an attempt to solve this problem; in their implementation, Becker and Jürgens (1990) introduced a cross-coupling between the input of the pulse-generators (Fig. 1*C*, *arrow 1*). In this case, the input to the pulse

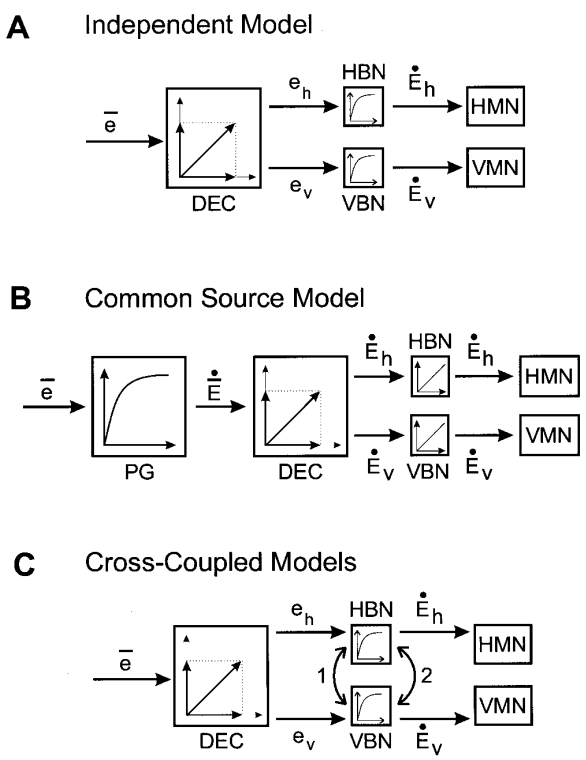

FIG. 1. Schematic representations of 2-dimensional models of saccadic system. Only feedforward path is shown. $\bar{e}$, vectorial motor error; e_h, horizontal motor error; e_v, vertical motor error; $\dot{\bar{E}}$, vectorial velocity command; $\dot{E}_h$, horizontal velocity command; $\dot{E}_v$, vertical velocity command; DEC, decomposition of the vectorial signal into its horizontal and vertical components; PG, vectorial pulse generator; MLBN, medium lead burst neuron; HBN, horizontal MLBNs; VBN, vertical MLBNs; HMN, motoneurons driving horizontal muscles; VMN, motoneurons driving vertical muscles. *A*: independent model. *B*: common source model. *C*: cross-coupled models. *Arrow 1*: mutual cross-coupling of motor errors. *Arrow 2*: mutual modulation of the gains. In *A* and *C*, pulse generation is accomplished by MLBNs.

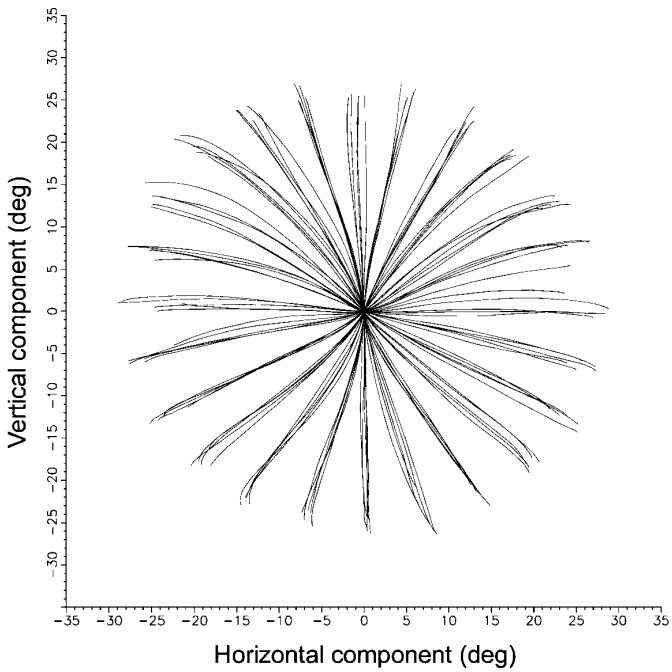

FIG. 2. Family of primate visually guided saccades (30° movements). Eye movements were recorded with magnetic field-search coil technique (Robinson 1963). Note that curvature is dependent on direction. Courtesy of Dr. H. Aizawa.

generators is not simply the motor error in one cardinal direction (vertical or horizontal), but is that quantity attenuated by a factor proportional to the motor error in the orthogonal component. With an appropriate choice of the cross-couplings, this model solves the problems that affected the Grossman-Robinson model.

One problem with all coupling models is that they offer no explanation for why the two burst generators should be coupled, other than to obtain straight saccades. The primary goal of the saccadic system should be to redirect the gaze as quickly as possible because of the known lack of vision during saccades (Carpenter 1988). Thus there would be no benefit from making straight, and slower, saccades rather than curved, and faster, saccades. Furthermore, many saccades are not straight. This residual curvature cannot be due to a lack of training, given that we make something like three saccades per second throughout our life, almost all of which are oblique. Thus if our brain developed cross-coupling to straighten saccades, it did a pretty bad job!

Physiological properties of MLBNs

A more serious problem for all these models, unrelated to the characteristics of oblique saccades described above, is that the vectorial signal generated by the premotor structures is decomposed into two orthogonal commands at the level of the medium lead burst neurons (MLBNs). That decomposition is explicit, because each neuron is activated in proportion to the cosine (for horizontal MLBNs) or sine (for vertical MLBNs) of the angle of the vectorial signal. Thus simulations of these models show activity in their horizontal MLBN during horizontal but not vertical movements (Fig. 3*A*). However, there is compelling physiological evidence that the output of single MLBNs is neither proportional to the horizontal nor to the vertical motor error (Kaneko et al. 1981; King and Fuchs 1979; Moschovakis and Highstein 1994; Moschovakis et al. 1991a,b; Scudder et al. 1988; Strassman et al. 1986a,b; Van Gisbergen et al. 1981). Furthermore, Van Gisbergen and colleagues (1981) studied burst neurons exerting an excitatory effect on abducens motoneurons projecting to the lateral rectus muscle and thus supposedly driven by the horizontal motor error. They showed that these MLBNs, having a relationship between motor error and their activity for horizontal saccades, also discharged vigorously for movements in the vertical direction (Fig. 3*B*). More importantly, many studies (Moschovakis and Highstein 1994; Moschovakis et al. 1991a,b; Scudder et al. 1988; Strassman et al. 1986a,b) have pointed out that each MLBN has its own on-direction (i.e., the direction of a movement associated with the largest number of spikes), that can be tilted away from the supposed on-direction [horizontal for MLBNs in the paramedian pontine reticular formation (PPRF) and vertical for MLBNs in the rostral interstitial nucleus of the medial longitudinal fasciculus (riMLF)] by as much as 70° (see Strassman et al. 1986a, their Fig. 4). Thus the on-direction of the MLBNs that drive the horizontal motoneurons can have a large vertical component that may be either up or down. The tuning curve of MLBNs (obtained counting the number of spikes produced during movements of the same amplitude in different directions) is broad and can be fit by a Gaussian function centered around the on-direction [which when plotted in polar coordinates is similar to a cardioid (e.g., Scudder et al. 1988, their Fig. 9)].

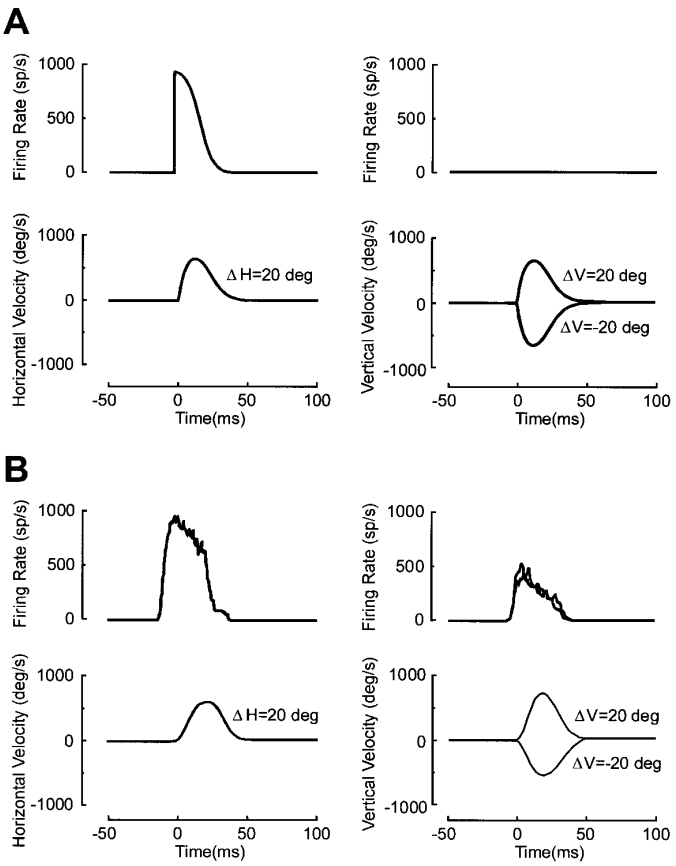

FIG. 3. Firing rate of horizontal MLBNs during purely horizontal and vertical movements. *A, top*: activity simulated using any of models described in Fig. 1, during a horizontal (*left*) or vertical (*right*) 20° movement. *Bottom*: velocity profiles of movements simulated. Note that there is no activity in MLBNs during vertical saccades. *B, top*: activity recorded in a MLBN of a behaving monkey during either horizontal (*left*) or vertical (*right*) eye movements. *Bottom*: velocity profiles of corresponding movements. Note presence of activity in MLBNs for horizontal and vertical (both upward and downward) saccades. Adapted from (Van Gisbergen et al. 1981).

It is important to stress that these properties of MLBNs cannot be explained simply by proposing that the pulse generators produce an output even for a null or negative motor error in their theoretical on-direction as often suggested (Tweed and Vilis 1985; Van Gisbergen et al. 1981). Whereas this could be an acceptable explanation for a MLBN having a horizontal on-direction, it does not hold for a neuron with an on-direction tilted away, say 60° upward, from the horizontal direction. A neuron like that would discharge differently in situations where the horizontal motor error is the same but the vertical motor error is different. For example, it would discharge more intensely for an error of 20° in its on-direction (horizontal motor error equal to 10°, Fig. 4, arrow A) than for an error of 20° in the horizontal direction (Fig. 4, arrow B) or for a saccade with the same horizontal component but pointed downward (Fig. 4, arrow C).

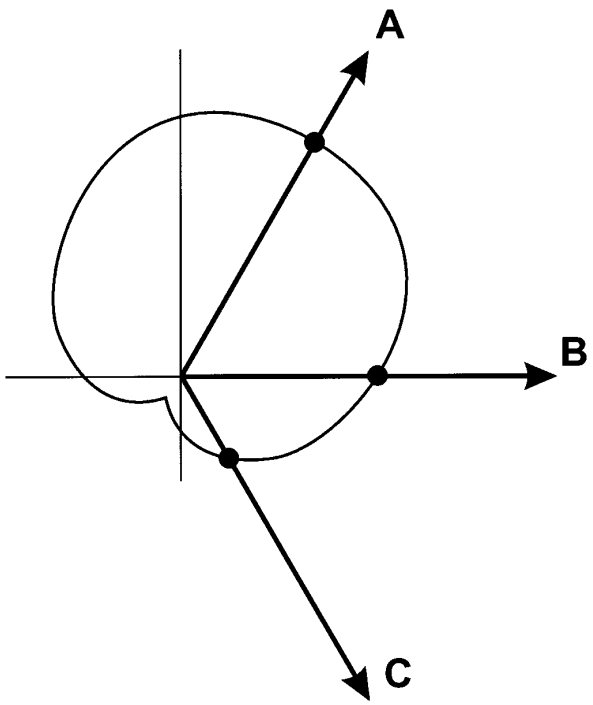

FIG. 4. Polar plot of activity generated by a simulated MLBN projecting to horizontal motoneurons but having an on-direction 60° above horizontal axis. Length of line segments from origin to ● where the arrows intersect the tuning curve shows amount of activity elicited during movements characterized by same vectorial amplitude (20°) but by a different direction (θ). When θ is equal to 60° (arrow A, horizontal component h = 10°), during movement cell discharges, for example, 40 spikes. For a horizontal movement (arrow B, θ = 0°, h = 20°), the cell produces 30 spikes. When θ is equal to −60° (arrow C, h = 10°), the cell produces only 13 spikes.

All these aspects of the MLBNs' activity during saccadic eye movements lead us to infer that the output of individual MLBNs cannot simply be viewed as the decomposition of a vectorial signal into its horizontal and vertical components.

MLBNs in early models of oblique saccades

None of the models of oblique saccades described above dealt with either the breadth of the tuning curve or the distribution of on-directions of MLBNs. In particular, all those models are lumped; i.e., they use an equivalent neuron, having a well-defined tuning curve with either a horizontal or vertical on-direction, and assume that all the neurons that compose a population of MLBNs behave in the same way. What distinguishes one model from another can be characterized by the shape of that tuning curve. To compare our model and previous models of the saccadic system, it is necessary to look at the different models from the same point view. Thus we will briefly describe the tuning curves of the independent, common source, and cross-coupled models.

MLBN TUNING CURVES OF EARLY MODELS. In the common source model (Fig. 1*B*), given a vectorial motor error described in terms of its magnitude e and its angle θ, a vectorial pulse is produced by a nonlinear pulse generator; the input-output relation of the pulse generator is described by

$$f(e) = A_0\left[1 - \exp\left(\frac{-e}{K_0}\right)\right] \qquad (1)$$

where A_0 is the saturation value and K_0 is a magnitude scaling factor. To obtain the horizontal drive, the vectorial pulse then is multiplied by the cosine of the angle θ. Thus the instantaneous firing rate of the horizontal burst neuron (recall that this is a lumped model) for a motor error (e, θ), normalized with the firing rate of the same neuron when the motor error is $(e, 0)$, is

$$R(\theta) = \frac{A_0\left[1 - \exp\left(\frac{-e}{K_0}\right)\right]\cdot\cos(\theta)}{A_0\left[1 - \exp\left(\frac{-e}{K_0}\right)\right]} = \cos(\theta) \qquad (2)$$

Under these circumstances, there is clearly no activity in the horizontal burst neuron for vertical eye movements [cos (90°) = 0], and the tuning curve, plotted in polar coordinates, is a circle (Fig. 5, solid curve). Moreover, because no nonlinear operation is applied to the decomposed signals, the tuning curve does not depend on the transfer function of the pulse generator and the ratio between the activity of the vertical and horizontal motoneurons is always equal to the tangent of θ; thus all the movements are straight.

In the case of the independent model (Fig. 1*A*), the tuning curve depends on the nonlinearity used. In this model, the vectorial motor error (e, θ) is decomposed immediately into its horizontal and vertical components (e_h and e_v, respectively), by multiplying e by the cosine and the sine of θ, respectively. To produce the horizontal drive to the motoneurons that project to the lateral rectus, the horizontal pulse generator applies to e_h the nonlinear function described in *Eq. 1*, with e_h instead of e. In this case, the instantaneous firing rate of the horizontal burst neuron for a motor error

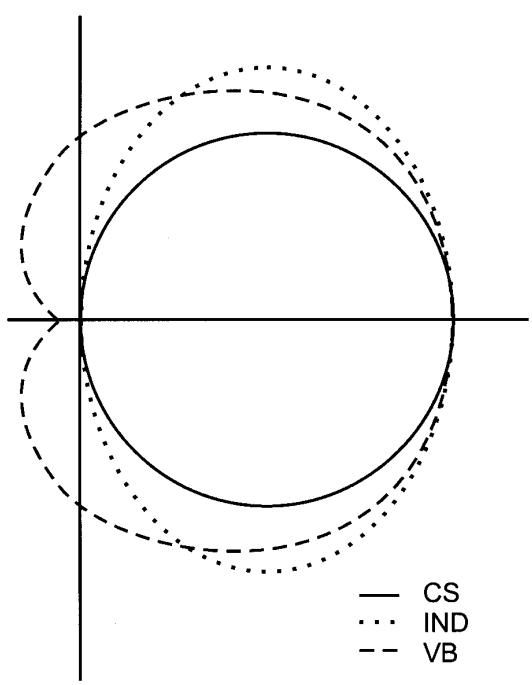

FIG. 5. Tuning curves of MLBNs implemented in 2-dimensional models of saccadic system. ——, CS model; · · ·, independent (IND) model; – – –, vectorial burster (VB) model. Tuning curves of cross-coupled models would lie between those of CS and IND models. Note that only VB model's tuning curve is not zero for vertical and off-direction movements.

(e, θ), again normalized with the firing rate of the same neuron when the motor error is $(e, 0)$, is

$$R(\theta) = \frac{A_0\left[1 - \exp\left(-\frac{e \cdot \cos(\theta)}{K_0}\right)\right]}{A_0\left[1 - \exp\left(-\frac{e}{K_0}\right)\right]} \quad (3)$$

Given *Eq. 3* and a vectorial error e, the exact shape of the tuning curve depends on the value assigned to K_0. If $K_0 \rightarrow 0$, $R(\theta) \rightarrow 1$, and the tuning curve is a semicircle centered on the origin; on the other hand, if $K_0 \rightarrow \infty$, $R(\theta) \rightarrow \cos(\theta)$ (this can be easily verified by expressing the exponential as a series or by using L'Hospital's rule) and the tuning curve is a circle. For values of K_0, in between these two extremes, the tuning curve varies correspondingly; in Fig. 5 (dotted curve), the tuning curve obtained for $e = 20°$ and $K_0 = 8°$ is shown. Note that in this model, for a vertical movement ($e_h = 0$), no activity is produced by the horizontal burst neurons. Furthermore, the two components are clearly independent (the ratio between the two is not forced to be equal to the tangent of θ, unless K_0 is very large), and the trajectory can be curved.

With the cross-coupled models (Fig. 1*C*), it is possible to obtain any desired tuning curve shape ranging from that of the common source to that of the independent model simply by changing the strength of the couplings; clearly, to obtain almost straight movements, an almost circular tuning curve is needed. Nonetheless, even these models cannot predict an activation of the horizontal pulse generator during a vertical movement (Fig. 3*A*).

It is important to stress that the different behavior of all the models considered above is not related in any way to the nature of the feedback loop (vectorial or independent for the two components); what counts is only the presence or absence (and, in the first case, the nature) of a nonlinear operation after the decomposition of the signal (either vectorial motor error or vectorial pulse) into horizontal and vertical components.

STATIC AND DYNAMIC TUNING CURVES. It is necessary to point out a fundamental difference between the tuning curve of the MLBNs described by Scudder and colleagues (1988), which we call static, and the tuning curves that we just analyzed, which we call dynamic. Static tuning curves are obtained by counting all the spikes produced during a movement, whereas dynamic tuning curves are obtained by measuring the instantaneous firing rate of a cell at a given time after saccade onset. The two curves could be different because the discharge of a cell may be shaped by a feedback signal. If we consider a lumped model, the static tuning curve reflects the accuracy of the saccadic endpoint and so should be essentially a circle. In contrast, the dynamic curve reflects the curvature of the trajectory and so could be noncircular. However, we think that there are good reasons to assume that the static and the dynamic tuning curves of MLBNs are similar. First, saccades are fairly straight, and so the feedback is probably more concerned with the control of the amplitude than the direction. Moreover, the activity recorded in PPRF MLBNs during vertical movement has a time course that is similar to the time course observed for a horizontal movement of the same amplitude.

New model

A new model, using MLBNs with Gaussian tuning-curves (both static and dynamic), and with a wide span of on-directions, is proposed here. We will demonstrate that this model, which is consistent with physiological recordings in the MLBNs, can generate, with the same set of parameters, cardinal movements that lie on the main sequence and oblique movements with an almost straight trajectory. Whereas in previous models the decomposition of vectorial signals into horizontal and vertical commands occurred explicitly at the level of individual premotor neurons (MLBNs), we propose that this decomposition occurs only at the motor level (motoneurons or plant), where the activity of all the MLBNs is algebraically summed. The decomposition occurs simply because the output of the motoneurons directly drives the extraocular muscles and is thus implicit in the model's structure rather than being explicitly accomplished by sets of sinusoidal weights at premotor levels.

We also will show that the stretching observed during oblique movements, which is not guaranteed by a decomposition, is simply a side effect of the organization and of the tuning curves of the MLBNs and does not reflect a strategy of trajectory control. In fact, the best arrangement for accomplishing the task that the brain delegates to the saccadic system (most rapid gaze shift) would be that described by the independent model. However, that would require an explicit (cosine, sine) decomposition of the motor error signal. We propose that the system does not perform this explicit decomposition perhaps because of its complexity or susceptibility to noise; instead, we propose that the saccadic system avoids this explicit process, using directional bursters characterized by a Gaussian tuning curve. The stretching then emerges because the ensemble average of individual tuning curves of the MLBNs is a circle when both ipsilateral and contralateral contributions are algebraically summed.

Prior models were lumped, because they used a single MLBN with an average tuning curve. This new model is distributed, because we consider a population of MLBNs each with its own tuning curve. We will discuss below how this distributed model of the premotor neurons imposes dramatic constraints on the organization of the whole saccadic system. In particular, we will demonstrate that, with the adoption of a distributed model for the burst generators, many of the structural and functional solutions that had been proposed for lumped models become meaningless, thereby forcing a change in the structure of many other parts of the system. Thus in an attempt to find a solution for the inconsistencies highlighted by our model of oblique saccade generation, we also will propose some new ideas about the general organization of the saccadic system. A brief description of this model appeared earlier (Quaia and Optican 1996).

METHODS

MLBN tuning curve

In our model, which we call the vectorial burster model (VB), a vectorial pulse is generated by applying *Eq. 1* to the vectorial motor error, as in the common source model. Thus in both these models, the tuning curve does not depend on the particular nonlin-

ear transfer function of the pulse generator. However, at this point in the VB model, the vectorial pulse is not decomposed into horizontal and vertical pulses by means of a (cosine, sine) decomposition. Instead, in our model each horizontal MLBN has a Gaussian tuning curve that is described by the equation

$$R(\theta) = \exp\left(-\frac{\theta^2}{2\sigma^2}\right) \quad (4)$$

A choice of $\sigma = 80°$ accounts fairly well for the observed activity of MLBNs (see Scudder et al. 1988, their Fig. 9); when plotted in polar coordinates the tuning curve (Fig. 5, dashed curve) is thus similar to a cardioid. The intercept of this tuning curve with the vertical axis is not zero, which implies that the activity for a vertical movement is not zero. Another important aspect of our tuning curve is that it predicts some activity even for movements in the opposite hemifield; with such a tuning curve, it is extremely important to account not only for the excitatory effect that ipsilateral MLBNs exert on the motoneurons but also for the inhibitory effect exerted by contralateral MLBNs. During a movement, two populations of MLBNs [ipsilateral excitatory burst neurons (EBNs) and contralateral inhibitory burst neurons (IBNs)] work in push-pull; for this reason, during a vertical movement, their net effect is zero, and there is no burst of activity in the motoneurons controlling the horizontal muscles.

MLBN on-direction

Another extremely important aspect of the physiology of MLBNs, not considered in previous models, which had only horizontal and vertical bursters (Fig. 6*A*), is that each neuron is characterized by a different on-direction. As already pointed out in the introduction, the on-direction of a neuron that excites the motoneurons of the lateral rectus of the right eye (the muscle that pulls that eye to the right) is always in the right hemifield, but can be tilted away from the horizontal rightward direction (the on-direction of the motoneuron) by as much as 70° (see, for example, Strassman et al. 1986a, their Fig. 4). Consequently, it is very important for a model to account for the fact that the MLBN population consists of a set of subpopulations of neurons, each with its own on-direction (Fig. 6*B*). The general equation describing the tuning curve of a MLBN characterized by an on-direction ψ is then

$$R_\psi(\theta) = \exp\left[-\frac{(\theta - \psi)^2}{2\sigma^2}\right] \quad (5)$$

Structure of the model

The overall structure of the feed-forward pathway of the VB model implemented here is represented in Fig. 7. The instantaneous vectorial motor error ($\vec{e}$) is computed by subtracting the horizontal and vertical displacements from the initial desired displacement; then, as in the common source model, a vectorial pulse ($\vec{D}$) is computed, using the nonlinear function described in *Eq. 1*, with $A_0 = 1{,}000$ spikes/s and $K_0 = 8°$. Taking into account the direction of the vectorial pulse and the tuning curve of the neuron, the output of each MLBN is evaluated by multiplying the magnitude of the vectorial pulse by $R_\psi(\theta)$, computed using *Eq. 5*. Thus here the on-direction (which determines the tuning curve) is a characteristic of the neuron. This is a simplification, because the differential projections from spatially organized structures (e.g., the superior colliculus) to the MLBNs presumably give rise to the MLBNs' tuning curves. Moreover, we do not consider separate populations of inhibitory MLBNs (IBNs) and excitatory MLBNs (EBNs). In fact, aside from the effect that they exert on motoneurons (excitation or inhibition) and their projections (ipsilateral for EBNs and contralateral for IBNs, in the case of MLBNs located in the PPRF), no clear physiological differences have been found between EBNs and IBNs. Thus we do not distinguish between EBNs and IBNs, and so we have only four populations of MLBNs (left, right, up, and down), exerting an opposite effect (excitation or inhibition) on the muscles of an agonist-antagonist pair. All the MLBNs converge to the motoneurons, where their activity is summed algebraically, accounting for their excitatory (agonist, solid lines) or inhibitory (antagonist, dotted lines) action. The tuning curve of the motoneuron is then very similar to a circle; this means that the smaller component has been stretched, and the saccades are almost straight (if the tuning curve were a circle, all saccades would be perfectly straight). The decomposition, which in the previous models was accomplished by appropriately weighted connections between the premotor structures (vectorially organized) and the MLBNs (where the signal was scalar, either horizontal or vertical), is here completely implicit; the projections from the MLBNs (where the innervational signal is not decomposed into horizontal and vertical signals) to the motoneurons all have the same weight. The decomposition is performed implicitly, simply because the output of a motoneuron, D_h or D_v, goes to only the horizontal or vertical muscles, respectively.

In our simulations, we used a lumped, linear plant, consisting simply of a horizontal and a vertical channel [modeled as a second order system, with time constants $\tau_1 = 0.15$ s and $\tau_2 = 0.05$ s (Keller and Robinson 1972; Robinson 1973)] not by agonist-

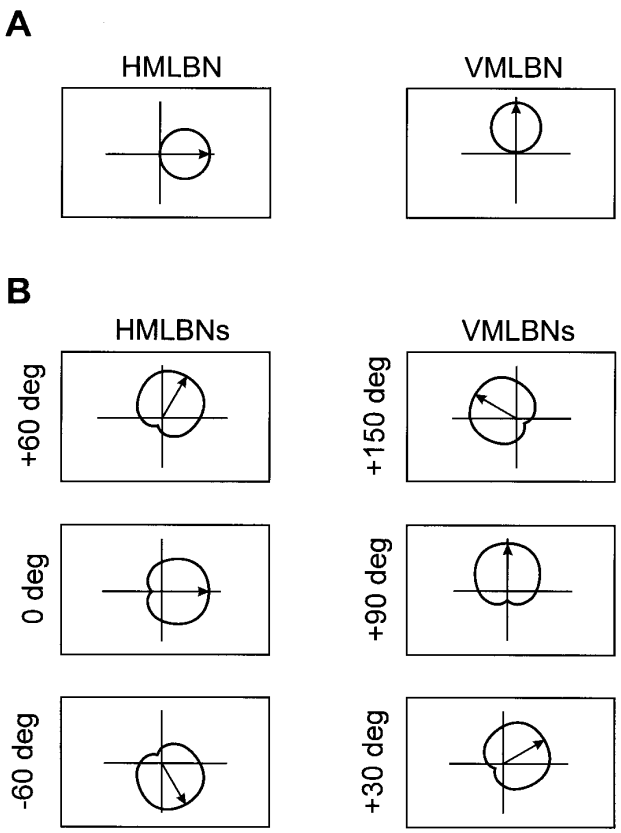

FIG. 6. Lumped and distributed MLBN models. HMLBNs, horizontal MLBNs; VMLBNs, vertical MLBNs. *A*: common source model uses only one tuning curve for all MLBNs that belong to one population of bursters (rightward, leftward, upward, or downward; only rightward and upward shown). Same is true for IND and cross-coupled models, with the only difference that tuning curve is not circular (cf. Fig. 5). *B*: VB model considers MLBNs with a wide span (120°) of on-directions. Thus different subpopulations, of neurons with the same on-direction, have to be considered within each population.

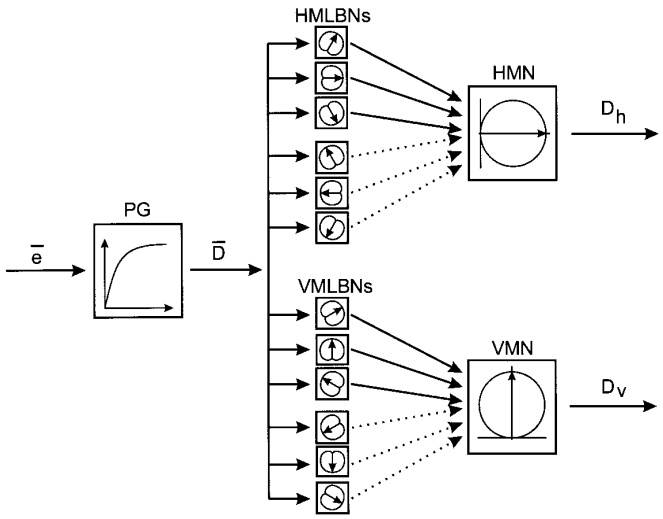

FIG. 7. Overall structure of the VB model implemented here. Only feedforward path is shown. $\bar{e}$, vectorial motor error; $\bar{D}$, vectorial drive; D_h, horizontal drive; D_v, vertical drive. In the implementation of the model, each population of MLBNs consists of 33 different neurons. Three neurons for each population are represented; → in each box indicates on-direction of Gaussian tuning curve of neuron (cf. Fig. 6*B*). Effect of summing activity of MLBNs is to produce an almost circular tuning curve for MNs.

antagonist pairs of muscles. This implies that the agonist/antagonist motoneurons have to be collapsed too. For this reason, in this model, the decomposition is accomplished, implicitly, at the level of the motoneurons. However, this does not exclude the possibility that the decomposition actually is carried out at an even lower level. This could happen directly at the level of the globe, where the force applied by the antagonist muscle is subtracted from that applied by the agonist muscle. Nonetheless, the simplification in the site of the decomposition affects neither the behavior of the model implemented here nor our conclusions.

Implementation of the model

The model was simulated using four populations of MLBNs, each consisting of 33 neurons, having uniformly spaced on-directions, spanning 120° around the primary on-direction (the on-direction of the motoneurons that receive an excitatory input from the population of MLBNs). We used the same sensitivity (i.e., the number of spikes per degree discharged during a saccade in their on-direction) for all our MLBNs, because there is no clear relationship between the on-direction of a neuron and its sensitivity (see Fig. 4 in Strassman et al. 1986a, where the sensitivity is represented by the length of the segments). To simulate the noninstantaneous rise of the MLBNs (see Fig. 3), we introduced a low-pass filter (τ = 2 ms) between the output of the pulse generator and the input of the MLBNs.

The model was simulated using MATLAB/SIMULINK (The Mathworks, Mass.) running on a Challenge-L computer (Silicon Graphics, California).

RESULTS

As already pointed out, there is a large variability in the curvature of oblique saccades. Thus we decided to concentrate on simulated MLBN activity rather than on simulated trajectories to differentiate among the models.

MLBN activity

In our model, the horizontal on-direction MLBNs must have some activity during a vertical movement because of the shape of the tuning curve. The first quantitative test for the model was to compare the activity of a MLBN having a horizontal on-direction during horizontal and vertical eye movements with the activity recorded in behaving monkeys (Van Gisbergen et al. 1981) in the same conditions. The result (Fig. 8) is clearly satisfactory, with a ratio between the activity elicited during a horizontal and a vertical movement very similar to that observed physiologically (Fig. 3B).

Component stretching

A critical characteristic of oblique eye movements is that the two components are stretched. It has been shown (Kaneko et al. 1981), by recording motoneurons' activity during cardinal and oblique movements, that this stretching is innervational, and not simply due to mechanical interactions. Thus the simulated activity of a MLBN must show the stretching. To test for this stretching, in Fig. 9*A* we have plotted the simulated activity of a MLBN with a horizontal on-direction, during movements having the same horizontal component (20°) but different vertical components. In this case, the shape of the tuning curve is not necessarily a good predictor of the observed activity. In fact, it is important to recall that the tuning curve compares the activity for movements in different directions but with the same amplitude, whereas in this case, the amplitude of the different movements is clearly not the same, ranging from 20 to 44.7°. Furthermore, in this case, the activity in all the MLBNs contributes to the shape of the MLBN that we are testing, because all the MLBNs contribute to define the motoneuron drive and thus the efferent copy of the motor command (used in the feedback loop to estimate the current eye displacement). However, from the simulation, it is clear that the pulse generated by our MLBN depends on the orthogonal component; when the vertical component is <20°, this effect is negligible, and the stretching is minimal, whereas when the other component becomes dominant (>20°), the stretching is much more pronounced, because the duration of the horizontal move-

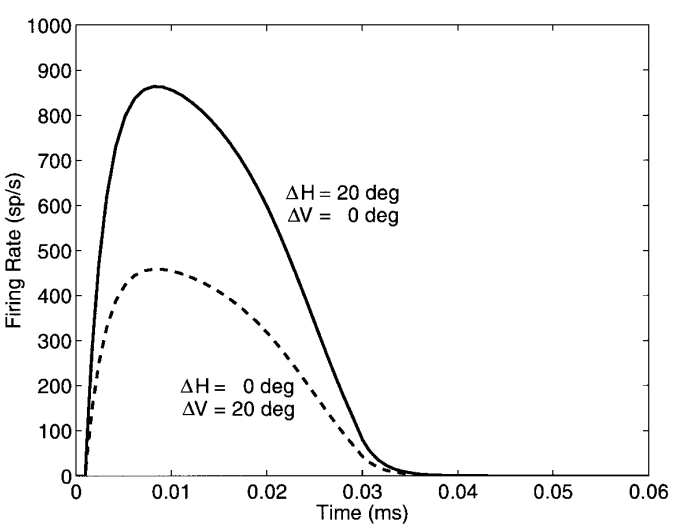

FIG. 8. Activity simulated by the VB model in a MLBN characterized by a purely horizontal on-direction during horizontal (——) and vertical (– – –) movements. This activity is similar to physiological recordings made under same conditions (Fig. 3*B*).

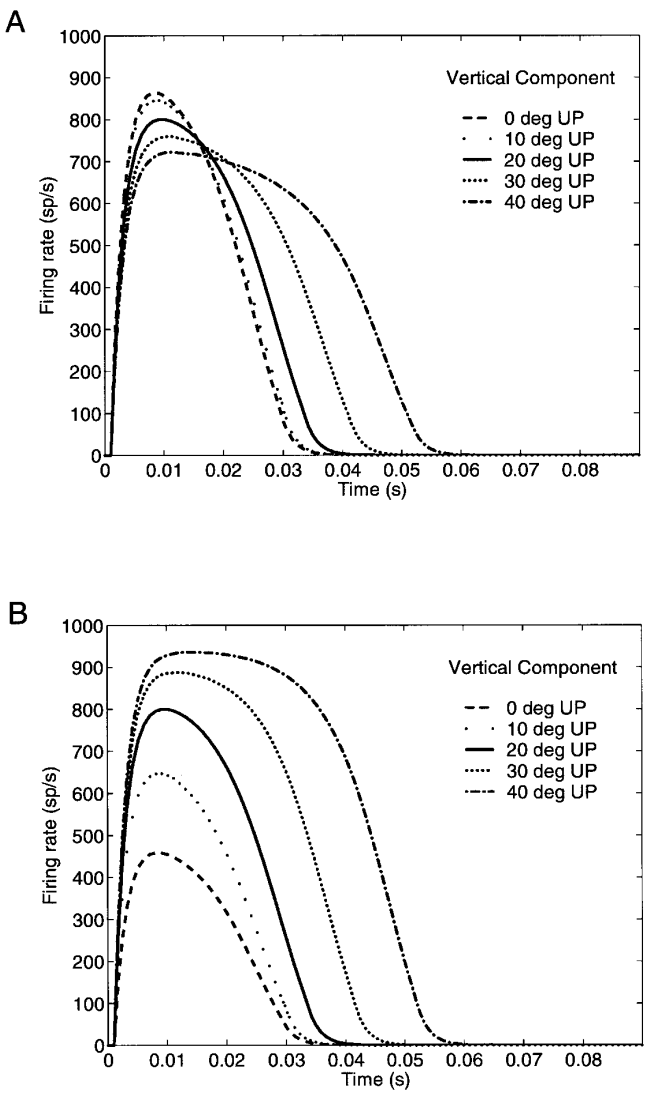

FIG. 9. Activity in MLBNs simulated by VB model during movements characterized by same horizontal component (20°) but with different vertical components (range 0–40°). (A) Activity in a MLBN having a purely horizontal on-direction. Activity is clearly affected by orthogonal component, and duration of burst is stretched. *B*: activity in a MLBN having a purely vertical on-direction. Comparing two panels, it is clear that for each movement, the smaller of two components is stretched so that duration of two bursts is always similar.

ment is increased to match that of the vertical component (Fig. 9*B*).

It is important to understand how our VB model stretches the smaller component. As we already recalled, the independent model does not predict any stretching in the components of an oblique movement because the horizontal and vertical channels are completely independent; thus to better understand the origin of the stretching predicted by our model, we compared the activity produced by the independent and by the VB models during an oblique movement (Fig. 10). In particular, we considered two movements: a rightward movement and a right-upward movement having the same amplitude. In Fig. 10*A*, the initial activity predicted by the independent model for the horizontal burst neuron is indicated by the number beside each arrow head. Normalizing the activity so that it is equal to 1 for the horizontal movement, an oblique movement elicits an activity of 0.7. This activity is applied directly to the horizontal motoneurons, determining the horizontal drive and, eventually, the force applied to the horizontal muscles. Now, to apply the same analysis to our model, we must consider that different subpopulations of neurons constitute the hori-

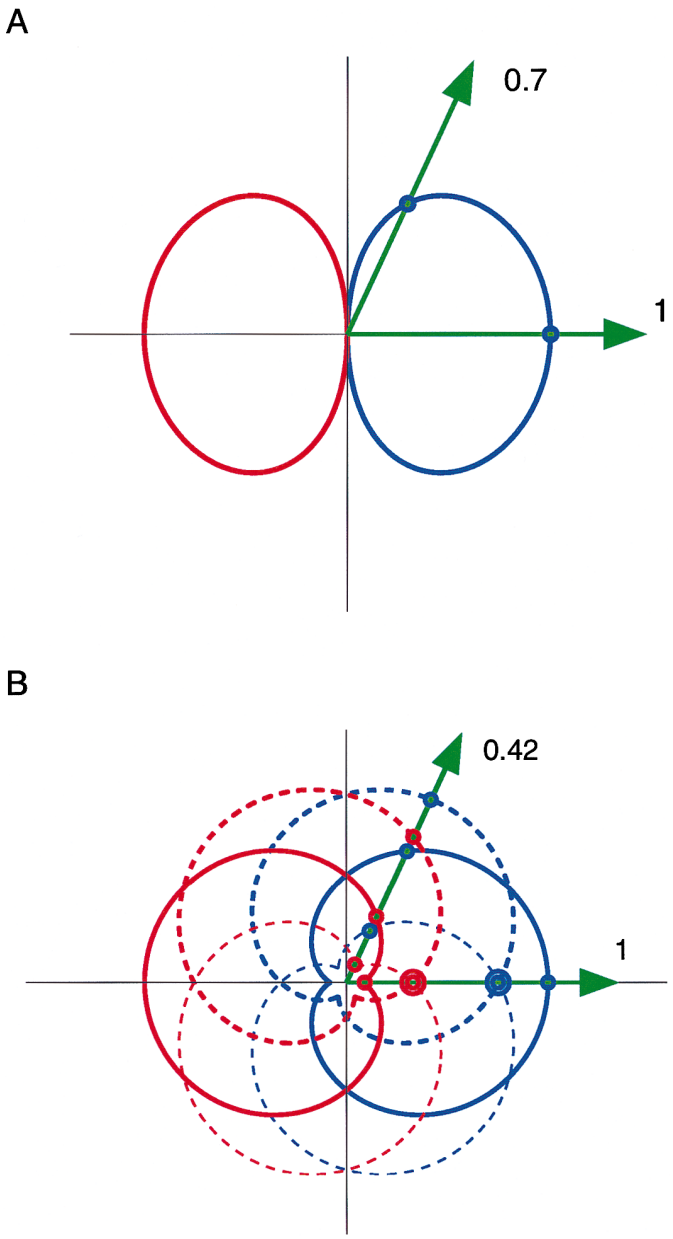

FIG. 10. Comparison of activity supplied by MLBNs to motoneurons of horizontal agonist muscle, as simulated by IND and VB models. Two movements with same vectorial amplitude are considered: one rightward and other right-upward. Length of segments from origin to ● placed at intersection of → and tuning curves indicates contribution of that neuron to total activity (blue, excitation; red, inhibition). In both panels, activity elicited during purely horizontal movement is normalized to 1. *A*: IND model predicts that activity during oblique movement is equal to 70% of activity associated with horizontal movement. *B*: in the case of VB model, same oblique movement is associated with a much lower drive (42%). Thus duration of horizontal component of oblique movement is longer in the case of VB model than with IND model, i.e., it is stretched.

zontal MLBNs population (in the example, we consider 3 neurons from each population). It is also necessary to account for both the ipsilateral (blue) and the contralateral (red) populations (Fig. 10*B*). On every arrow, we have put a circle where it intersects one of the tuning curves (representing different subpopulations of MLBNs); the circle is blue when the neuron is excitatory, red when it is inhibitory. After that, we algebraically summed the blue (+) and the red (−) points, and we normalized these sums, so that they were equal to 1 for a horizontal movement, as previously done for the independent model. The result is that the normalized drive produced by the horizontal motoneurons for the oblique movement is 0.42, much less than the 0.7 predicted by the independent model. This example clearly shows that the drive predicted by the VB model for one component of an oblique movement is much lower than that predicted by the independent model for the same component, and this is a very good indirect test of the observed stretching. The analysis in Fig. 10 leads to two major conclusions about the causes of the stretching. First, the level of activation of the subpopulations of burst neurons changes for movements in different directions; second, the inhibitory effect exerted by the contralateral population depends dramatically on the direction of the movement. In contrast, the effect of feedback is negligible.

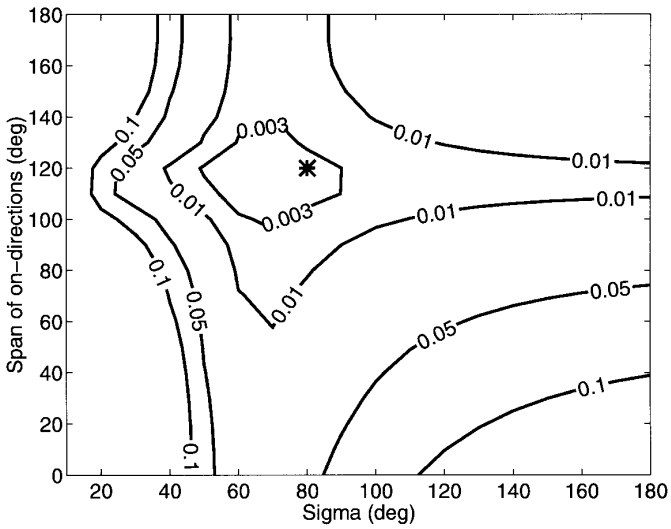

FIG. 11. Sensitivity of tuning curve of motoneurons on parameters used for MLBNs. Abscissa represents width of Gaussian tuning curve, whereas ordinate shows span of on-directions. Thirty-three neurons where used for each population. Deviation from circularity Δ (see text) is expressed in a contour plot. Level lines for 0.3, 1, 5, and 10% are plotted. Values used in simulations reported in paper (span = 120°, σ = 80°) (*) are nearly optimal for producing a circular tuning curve on motoneurons by summing Gaussian tuning curves of MLBNs.

Curvature

The curvature of a movement is determined by the difference between the initial (θ_i) and the overall (θ) direction of a movement. The overall direction depends only on the target position; if we indicate with T_h and T_v, the horizontal and vertical component of the target position (in retinotopic coordinates), it follows that

$$\tan(\theta) = \frac{T_v}{T_h}$$

On the other hand, the tangent of the initial direction is determined by the ratio between the vertical and the horizontal pulse applied, at the very beginning of the movement, to the plant. In other words, the initial direction depends on the relative drive applied to the motoneurons at saccade onset for a given target position. This drive is determined by the tuning curve of the motoneurons, which in turn is a function of the tuning curves of the MLBNs. Thus it is possible to evaluate analytically the tuning curve of the motoneurons, which in turn determines the degree of curvature (and of stretching) of the movements. With the MLBN tuning curves and the span of on-directions used in this model, the resulting tuning curves of the vertical and horizontal motoneurons are very close to sine and cosine functions (circles in polar coordinates). To test the sensitivity of the model on the parameters used, we computed the global tuning curve for different values of the span of on-directions (from 0 to 180°, uniformly distributed) and of the width of the Gaussian (σ from 10 to 180°). To estimate the departure from circularity of the global tuning curve, we have used the following measure of the distance between the two curves

$$\Delta = \sqrt{\frac{\int_{-90}^{+90} [\cos(\theta) - y(\theta)]^2 d\theta}{\int_{-90}^{+90} [\cos(\theta)]^2 d\theta}}$$

where $y(\theta)$ is the global tuning curve for the horizontal motoneuron. In Fig. 11, we show a contour plot with isodistance lines for values of Δ of 0.003 (0.3% of departure from circularity), 0.01 (1%), 0.05 (5%), and 0.1 (10%). It is interesting to note that the values used in the model (span = 120°, σ = 80°, * in Fig. 11), which have been extrapolated from the data, are nearly optimal for obtaining circularity across the ensemble; nonetheless, even large changes in these parameters have only small effects on the global tuning curve. When a Gaussian distribution of the on-directions is used instead of a uniform distribution, a very similar contour plot is obtained (with a minimum at σ = 70° for the tuning curve of the neuron and at σ = 50° for the distribution of on-directions).

Thus the saccades generated by the model are almost perfectly straight. However, this happened only because both the neural and mechanical components of the model were symmetric. If we introduce asymmetries in either the distribution of on-directions (Fig. 12*A*) or in the gain of the plant (Fig. 12*B*), the saccades become curved because there is no control of trajectory in the model. To obtain the results shown in Fig. 12*A*, we used on-directions distributed uniformly from −30 to 60°, instead of the original −60 to 60°, for the rightward EBN/IBN population. The saccades shown in Fig. 12*B* were obtained by reducing the gain of the horizontal channel of the plant by 30%. It is important to point out that there is experimental evidence for the presence of such asymmetries; for example, it is well known that saccades in different cardinal directions are characterized by different dynamic properties (Becker and Jürgens 1990),

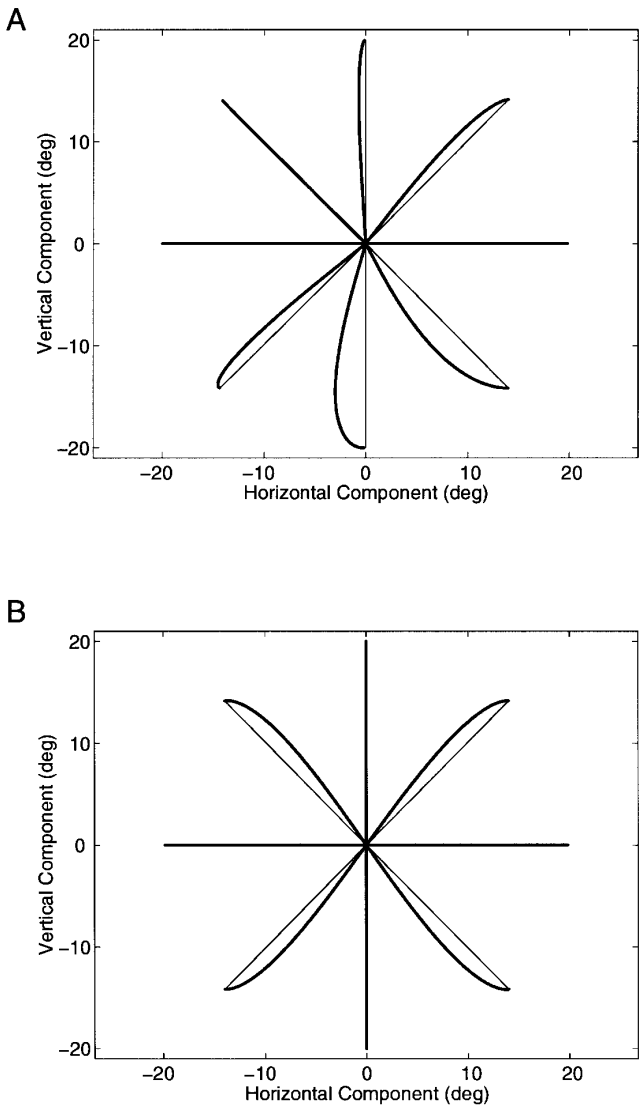

FIG. 12. Trajectories of simulated saccades. Because of tuning curves used, when neural and mechanical subsystems are symmetric, almost perfectly straight saccades are produced. However, if asymmetries are introduced, saccades become curved. *A*: trajectories obtained when on-directions of rightward EBN/IBN population span from −30 to 60°, instead of original (symmetric) −60 to 60°. *B*: trajectories obtained by reducing gain of horizontal channel of plant by 30%. Note that reducing mechanical gain leaves cardinal saccades straight.

although whether this is due to asymmetries in the neural signals and/or in the plant is not known.

DISCUSSION

From the physiological data acquired in the last 15 years by many groups, we infer that the brain does not perform an explicit decomposition of the premotor vectorial command into horizontal and vertical commands; this decomposition is probably accomplished, implicitly, at the level of the extraocular motoneurons. As pointed out by others (Hepp et al. 1989), different studies do not agree on the span of MLBNs' on-directions and some (e.g., Scudder et al. 1988) report a more restricted span than others (e.g., Strassman et al. 1986b). However, all the studies report at least one MLBN having an on-direction tilted away from the theoretical on-direction by as much as 40°, and this is more than sufficient to support the conclusion that no explicit decomposition takes place. Thus we have proposed a distributed model that does not perform an explicit decomposition, simulates the physiological pattern of activity recorded in the MLBNs, and shows component stretching; the stretching observed during oblique movements is an emergent property of the organization and tuning curve of the MLBNs.

Curvature

Another consequence of the organization proposed here for the burst generators is that simple asymmetries in the distribution of the on-directions of MLBNs, or differences in the shape of some tuning curves, can account very easily for the differences in curvature observed for movements in different directions in the same subject (cf. Fig. 2), as well as for intersubject and interspecies differences in curvature. However, once the parameters of the model have been chosen, the curvature of the trajectory for a given movement is determined and does not vary. To account for the observed variability in the initial direction (and, thus, curvature) of saccades made by the same subject between the same two fixation points (identical desired displacement) (Erkelens and Sloot 1995; Erkelens and Vogels 1995), we must introduce an additional degree of freedom in our model. This could be accomplished easily by hypothesizing transient changes in the gain of MLBNs, possibly due to fluctuations of the inhibitory effect exerted by omnipause neurons. Alternatively, this variability could be the effect of a change in the input supplied by premotor structures to the MLBNs (see below). In particular, the latter speculation is supported by the finding (Aizawa and Wurtz 1994; Hikosaka and Wurtz 1985) that temporary lesions of the superior colliculus (SC) can cause dramatic alterations in the trajectory of a movement with relatively little effect on the accuracy of the movement itself.

Comparison with the original common source model

Given the vectorial nature of its pulse generator, the VB model presented here can be considered as a variant of the common source (CS) model. The most important difference between the VB and the other CS models is obviously that the former does not involve an explicit decomposition of the collicular signal into horizontal and vertical commands. In contrast, the originally proposed CS models used weights related to the cosine and the sine of the elevation angle; unless these weights are determined genetically, they would need to be learned by the system. However, if the output of the SC is a velocity signal and not simply a desired displacement signal, the process of learning the weights would reflect a trajectory control (the controlled parameter is the ratio between the horizontal and vertical velocity, i.e., the direction of the movement), whereas, as we pointed out previously, there are many good reasons to suppose that such a control does not take place. Furthermore, Smit and coworkers (1990) proposed that asymmetries in the SC map could account for asymmetries in the stretching, and thus in curvature, for saccades in different directions; however, during

the learning of the weights of the SC-MLBNs' connections, such asymmetries would be taken into account, producing weights that would differ from the cosine and the sine of the elevation, compensating for the SC asymmetries and, eventually, leading to straight saccades in all the directions.

Stimulation experiments

Recently, it was reported (Nichols and Sparks 1996) that oblique saccades elicited by electrically stimulating sites in the superior colliculus immediately after the offset of a visually triggered saccade are almost straight. In that paper, the authors concluded that their results support a cross-coupled structure and are incompatible with a common-source structure. However, their results may be interpreted in another way that is compatible with a common-source structure. Their interpretation is based on the assumption that the excitatory input to the MLBNs is essentially the same whether the collicular stimulation is applied during fixation or just after a visually guided movement. The authors justify this assumption on the basis that it is reasonable to suppose that the SC output does not change in the two conditions. Thus they conclude that the stretching is due to interactions at the level of the MLBNs, as in cross-coupled models, and not to a change in the collicular locus activated, as in CS models. However, even if the SC output is the same, it is important to remember that other structures (e.g., the fastigial nuclei) are known to project to the MLBNs, presumably through excitatory connections. Recordings in those areas (see, for example, Fuchs et al. 1993) reveal that some of these structures exhibit a very different pattern of discharge during fixation and during the postsaccadic period; thus the excitatory input to the MLBNs may be very different in the two conditions. So, it is possible that the stretching observed arises because of the activity present in those other structures when the stimulation is applied and could have nothing to do with the mechanism that produces the stretching under physiological conditions.

Furthermore, we will show in the next section how the cross-coupled scheme has several problems when implemented in a distributed network and cannot easily account for the distribution of on-directions of MLBNs.

Organization of the saccadic system

This model was designed to explain observed behavioral and physiological data related to oblique saccades and MLBNs. The model, because of its distributed nature, also provides new insights into the general organization of the saccadic system.

INPUT TO THE MLBNS. In implementing this model, we assumed that the on-direction and the directional tuning are characteristics that belong to each neuron; clearly this assumption, even if reasonable from the point of view of the implementation of the model, is extremely unphysiological. The best possible hypothesis is that these characteristics both emerge as a consequence of the inputs that each MLBN receives. For a long time, the long lead burst neurons (LLBNs) have been considered as an intermediate stage, organized in semipolar coordinates, between the SC, where the signal is in polar coordinates, and the MLBNs, where the signal was assumed to be decomposed into Cartesian coordinates. However, there appears to be no significant difference between the tuning curve and the span of on-directions for MLBNs and LLBNs (Scudder et al. 1988). Given the lack of decomposition and the extreme similarities between LLBNs and MLBNs, it is probably necessary to think of the LLBNs as involved in some other task, whereas the input to both the LLBNs and MLBNs could reasonably come directly from the SC. This hypothesis is supported by the recent finding, in the cat, that it is possible to activate monosynaptically the MLBNs from the SC (Chimoto et al. 1996). The tuning curve of MLBNs thus would be a consequence of the organization of the projections from the SC. Given the large amount of collicular activation during each saccade (Munoz and Wurtz 1995; Ottes et al. 1986), direct projections from the SC to the MLBNs are sufficient to explain the broad tuning curves of the MLBNs. It is important to point out that it would not be necessary for the projections from the SC to the MLBNs to have particular weights (e.g., sine or cosine of saccade elevation), because these projections would not be used to perform any kind of coordinate transformation of the premotor command; the only constraint would be that the part of the colliculi associated with values of θ around 0 and 180° should project preferentially to the horizontal populations of MLBNs (in the PPRF), whereas the collicular stripes associated with movements around 90 and 270° should project preferentially to the vertical populations of MLBNs (in the riMLF). These preferential projections could be determined genetically or could arise through learning. As pointed out previously, the goal of this learning cannot be to make saccades straight, as they are not perfectly straight. However, it is not known whether the saccadic system can achieve its goal of producing accurate movements in the presence of large curvatures. Thus it is possible that the learning process simply keeps the curvature of saccades within the range necessary for producing accurate movements.

FEEDBACK LOOP. Another very important structural feature of all saccade models that must be reconsidered, because of the distribution of physiological characteristics of MLBNs, is the internal velocity/position feedback loop. Feedback is straightforward to implement for lumped models but becomes extremely complex and contrived in more physiological, distributed, models. Thinking in terms of the classical feedback loop scheme (Fig. 13), as proposed by Robinson (Robinson 1975) and subsequently modified by Jürgens and coworkers (Jürgens et al. 1981), several questions arise: which signal is used as the efference copy of the motor command? Where is the current displacement subtracted from the desired displacement signal? At what level does the pulse generation take place?

Physiologically, the motor command is present in the system only at the level of the motoneurons; however, the motoneurons are outside the feedback loop, because the effects of a stimulation delivered to the motoneurons during an eye movement are not compensated (Sparks et al. 1987). This implies that the feedback signal must be obtained by reconstructing, somewhere, the signal that is supplied to the motoneurons. Thus all the burst neurons that project to the motoneurons, or at least a significant subset of them, must contrib-

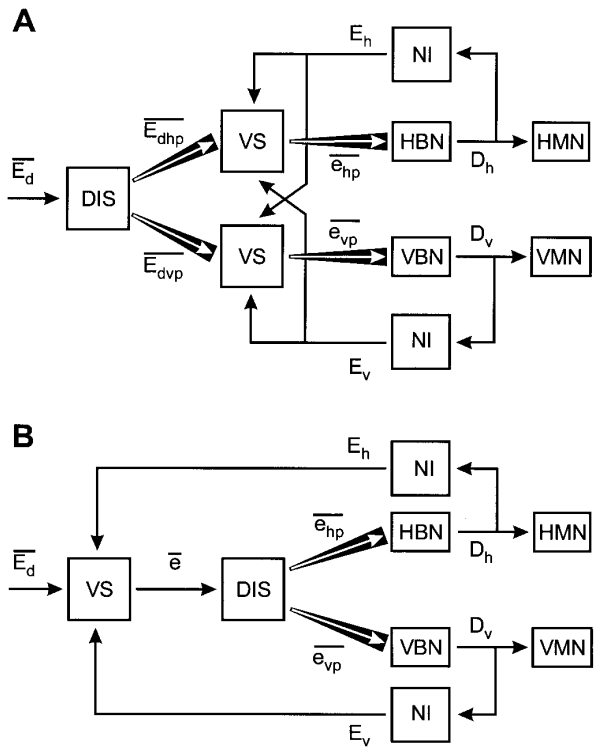

FIG. 13. Schematic representation of possible implementations of distributed version of feedback loop in saccadic system. In both cases, input to MLBNs encodes residual motor error, as proposed by Robinson model (Robinson 1975). $\bar{E}_d$, desired vectorial eye displacement; $\bar{E}_{dhp}$, desired eye displacement distributed to horizontal population of MLBNs; $\bar{E}_{dvp}$, desired eye displacement distributed to vertical population of MLBNs; $\bar{e}$, vectorial motor error; $\bar{e}_{hp}$, residual motor error for horizontal population of MLBNs; $\bar{e}_{vp}$, residual motor error for vertical population of MLBNs; D_h, horizontal drive; D_v, vertical drive; E_h, estimate of horizontal eye displacement; E_v, estimate of vertical eye displacement; DIS, distribution of vectorial signal to horizontal and vertical populations of MLBNs; VS, vectorial summing junction; HBN, horizontal MLBNs; VBN, vertical MLBNs; HMN, motoneurons driving horizontal muscles; VMN, motoneurons driving vertical muscles; NI, neural integrator. White arrows on black background indicate distributed signals. *A*: current displacement is subtracted from desired displacement at level of MLBNs. Feedback signal consists of horizontal and vertical components of displacement, whereas on-directions of MLBNs range widely around cardinal directions. Thus for each MLBN, correct current displacement signal must be generated by summing appropriately the horizontal and vertical components of feedback signal. *B*: alternatively, estimates of horizontal and vertical displacement could be fed directly to upper centers (like superior colliculus), where a vectorial summation would be performed. Note that there is no explicit decomposition of vectorial premotor signal into its horizontal and vertical components; vectorial signal is distributed simply to different populations of MLBNs, according to on-direction of each MLBN and to its tuning-curve.

ute to the efference copy signal; in particular both ipsilateral and contralateral MLBNs must be considered (with opposite effect). Irrespective of their on-direction, the MLBNs project only to horizontal and vertical motoneurons, and thus their output must be considered part of the horizontal or vertical efference copy of the command. Thus all the MLBNs in the PPRF must project to the horizontal displacement integrator (with ipsilateral excitation and contralateral inhibition), and all the MLBNs located in the riMLF must project to the vertical displacement integrator.

Now consider the hypothesis that the displacement signal is subtracted from the desired displacement at the level of the MLBNs (Fig. 13*A*). We have described (Fig. 6*B*) MLBNs in the PPRF with an on-direction far away from the horizontal axis; this means that their activity is related essentially to the value of the motor error in an oblique direction rather than in the horizontal direction. This implies that the vectorial desired displacement ($\bar{E}_d$) is not decomposed into its horizontal and vertical components, but is simply distributed (DIS) to the horizontal and vertical populations of MLBNs. Each MLBN population will receive a family of inputs ($\bar{E}_{dhp}$ and $\bar{E}_{dvp}$). Each neuron of a population will have a different on-direction, depending on which inputs contact the neuron. Now, if an MLBN receives from the premotor circuits (say the SC) an excitatory input mainly proportional to the desired displacement in one direction ψ, it also must receive from the feedback branch an inhibitory input that is encoded in the same framework, i.e., an estimation of the displacement of the eyes in the direction ψ. Unfortunately, as we just pointed out, the system does not have such a signal available, and thus it would have to generate it, vectorially summing together (VS), with the proper weights, the estimates of the horizontal (E_h) and vertical (E_v) displacements, thus performing an inverse coordinate transformation. This transformation would be different for each MLBN depending on its on-direction. This scheme raises many questions. Why would the system avoid performing a decomposition into Cartesian coordinates in the feedforward path but then execute a more complicated inverse transformation in the feedback path? How can the appropriate weights be learned given the strong convergence from MLBNs to motoneurons? How can such an arrangement account for the broad tuning of the neurons? Even if this scheme could compute a feedback signal for each on-direction, how would that explain the decay of activity observed (see Fig. 3*B*) during a movement orthogonal to the on-direction of the cell (when there is no displacement along the on-direction and thus no inhibitory feedback)?

All these unanswered questions make it doubtful that such a scheme is correct. One possible alternative, compatible with the classical feedback loop idea, is that the evaluation of the current motor error is not accomplished by the MLBNs in a temporal framework but in upstream premotor structures, such as the SC, where the signals are organized in a spatial framework. The most likely hypothesis is then that the premotor signal distributed (DIS) to the MLBNs is not simply the desired displacement ($\bar{E}_d$), but either the current motor error (Fig. 13*B*, $\bar{e}$) or the vectorial pulse itself (Fig. 14, *A* and *B*, $\bar{D}$). In these schemes, the SC is inside the feedback loop and embeds the vectorial summing junction (VS). In the first case (Fig. 13*B*), the SC simply acts as a summing junction, whereas in the other cases (Fig. 14) it also carries out the generation of the pulse. Every stripe along the rostral-caudal (constant direction) axis on the SC should project to a particular MLBN, thus determining its on-direction; unfortunately, it is impossible to determine the nature of the output of the SC (motor error or vectorial pulse) simply by looking at the activity recorded in the MLBNs. However, in both cases, the important point is that to have a change in direction (i.e., in the relative weight of the horizontal and vertical drive) and thus a curved trajectory, a change in the spatial distribution of activity along the medial-lateral (constant amplitude) axis in the SC must

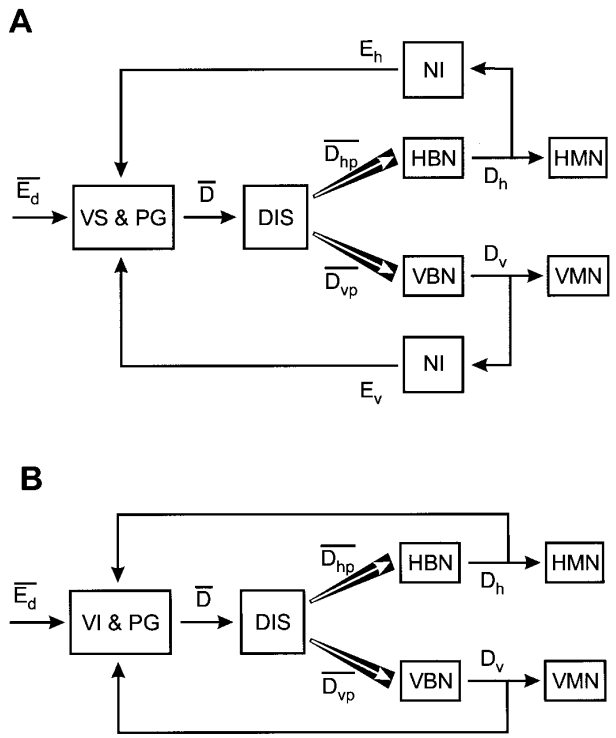

FIG. 14. Other implementations of distributed version of feedback loop. In these cases, MLBNs do not generate pulse from motor error signal but act merely as a relay station between superior centers and motoneurons. $\bar{D}$, vectorial drive; $\bar{D}_{hp}$, vectorial drive distributed to horizontal population of MLBNs; D_{vp}, vectorial drive distributed to vertical population of MLBNs; VS & PG, vectorial summation and pulse generation; VI&PG, vectorial integration and pulse generation; see Fig. 13 for other definitions. *A*: current displacement is evaluated in a pair of temporal neural integrators (one for horizontal and another for vertical component of displacement). Their outputs are fed to superior colliculus (SC), a spatially organized structure, where residual motor error is evaluated vectorially and corresponding pulse is generated. *B*: alternatively, estimates of horizontal and vertical drive could be fed directly to SC, where a vectorial integration would be performed to evaluate current motor error. Output of SC then would be a vectorial pulse that would be supplied to MLBNs. As in Fig. 13, no explicit decomposition is carried out by system.

occur. Even if it is acceptable to think that sudden, unpredictable changes in the gain of one population of MLBNs can be responsible for changes in the instantaneous direction of the movement (Becker and Jürgens 1990), it is impossible to justify the fact that such changes in direction are compensated and that eventually the eye is brought on the target, unless a shift of the center of activity on the SC map is hypothesized. For this reason, models of the SC in which the change of the motor error (or of the drive to the MLBNs) is not represented by a change in the locus of activity on the collicular map but only by a change in the level of activation (Arai et al. 1994; Van Opstal and Kappen 1993; Waitzman et al. 1991) cannot predict the curvature of oblique saccades. Moreover, such models cannot deal with the observation that the two components of an oblique movement can end independently (Bahill and Stark 1977; Becker and Jürgens 1990; King et al. 1986).

Thus the only way to preserve the classical idea of the presence of a feedback loop that evaluates the current motor error and feeds it to a pulse generator, which in turn produces the velocity signal, is to embed, physically (Fig. 14*B*) or at least functionally (Figs. 13*B* and 14*A*), a spatial integrator in the SC, as has been proposed (Droulez and Berthoz 1988; Lefèvre and Galiana 1992; Optican 1994, 1995). In the schemes represented in Figs. 13*B* and 14*A*, the current horizontal (E_h) and vertical (E_v) displacements are evaluated by neural integrators (NI) outside the SC (position feedback). In the last case (Fig. 14*B*), a copy of the horizontal (D_h) and vertical (D_v) commands supplied to the motoneurons is vectorially integrated (VI) by the SC to evaluate the current motor error (velocity feedback). In these models, the efference signal is used to change the spatial distribution of the activity on the SC map in accordance with the residual motor error. However, several problems arise with such an arrangement. First of all, large lesions in the SC (Aizawa and Wurtz 1994) can affect profoundly the dynamical properties of movements (e.g., latency, peak velocity, initial direction), without any dramatic effect on saccadic accuracy, whereas it is obvious that the major effect of a lesion to the displacement integrator should be the presence of dysmetric movements. Furthermore, after SC ablation, the system can recover and within a few days can perform normal saccades. If the SC were the site of the saccadic integrator, recovery would require constructing a new integrator. Thus none of the models based on a local feedback loop proposed so far can explain all the properties of saccades.

DIFFERENT STRUCTURE FOR THE SACCADIC SYSTEM. We have shown here that the simple implementation of a distributed model with physiological elements has dramatic implications for modeling the whole saccadic system. In fact, when one part of the system is implemented in a distributed manner, all the parts that interact with it must be reconsidered. Solutions that made sense in a lumped framework may not make sense at all in a distributed framework. Starting from physiological findings, we have raised questions that make many of the solutions proposed in the past unusable. In particular, we have shown that the feedback loop itself is extremely difficult to implement. Thus it is not unreasonable to propose that a different structure may be used to achieve the same result as a feedback scheme, i.e., the accuracy of saccadic eye movements regardless of their velocity.

The arguments presented here suggest that the SC must do more than merely provide a target but less than tightly control the motoneurons' activity. It is reasonable to hypothesize that several different structures interact in the process of defining the drive supplied to the motoneurons. For example, cerebellar lesions are, to our knowledge, the only lesions that lead to enduring dysmetria, mainly hypermetria (Optican and Robinson 1980); thus it is extremely likely that the cerebellum plays a key role during the execution of saccades. To incorporate these observations, a model where both the SC and the cerebellum provide input to the MLBNs and uses a novel feedback scheme, was proposed recently (Optican et al. 1996).

It is important to stress that these observations on the feedback loop and on the role of the SC do not undermine the results obtained here regarding oblique saccades. In fact, the distribution of the on-directions of MLBNs on which we relied is a physiological reality and, as we have shown, can account by itself for the stretching and the mild curvature of oblique saccades.

CONCLUSIONS

We have demonstrated here that, using MLBNs that more closely resemble the activity actually recorded in primate neurons, a model can account easily for most of the properties of oblique saccades without introducing any arbitrary cross-couplings and/or structures whose only purpose would be to obtain straight saccades. In contrast, in our model the stretching is simply a side effect of the method adopted by the system to avoid an explicit decomposition of the premotor signals into two components; the residual curvature observed can be the result of asymmetries in the system. Having some curvature is perfectly reasonable for a side effect, whereas it is a sign of failure for a system designed to eliminate it.

We also have discussed the risk of drifting away from physiological reality when modifying lumped models to account for new observations. We suggest that it is time to abandon models that impute to a single structure all saccadic behavior. In fact, models that account for the interaction of different structures and that preserve the distributed nature of neural systems are not only more realistic but also may be necessary to explain how this intriguing system works.

We are grateful to Dr. Hiroshi Aizawa for providing the eye movement data for Fig. 2. We thank Drs. Robert H. Wurtz, David A. Robinson, Jan A. M. Van Gisbergen, and Philippe Lefèvre and an anonymous reviewer for helpful comments about the manuscript.

Address for reprint requests: L. M. Optican, Building 49, Room 2A50, National Eye Institute, National Institutes of Health, Bethesda, MD 20892-4435.

E-mail: loptican@nih.gov

Received 4 February 1997; accepted in final form 22 April 1997.

REFERENCES

AIZAWA, H. AND WURTZ, R. H. Control of trajectory of saccadic eye movements by monkey superior colliculus. *Soc. Neurosci. Abstr.* 20: 141, 1994.

ARAI, K., KELLER, E. L., AND EDELMAN, J. A. Two-dimensional neural network model of the primate saccadic system. *Neural Networks.* 7: 1115–1135, 1994.

BAHILL, A. T., CLARK, M. R., AND STARK, L. The main sequence: a tool for studying human eye movements. *Math. Biosci.* 24: 191–204, 1975.

BAHILL, A. T. AND STARK, L. Neurological control of horizontal and vertical components of oblique saccadic eye movements. *Math. Biosci.* 27: 287–298, 1975.

BAHILL, T. AND STARK, L. Oblique saccadic eye movements. *Arch. Ophthalmol.* 95: 1258–1261, 1977.

BALOH, R. W., SILLS, A. W., KUMLEY, W. E., AND HONRUBIA, V. Quantitative measurement of saccades amplitude, duration and velocity. *Neurology.* 25: 1065–1070, 1975.

BECKER, W. AND JÜRGENS, R. Human oblique saccades: quantitative analysis of the relation between horizontal and vertical components. *Vision Res.* 30: 893–920, 1990.

CARPENTER, R.H.M. *The Movements of the Eyes.* London: Pion, 1988.

CHIMOTO, S., IWAMOTO, Y., SHIMAZU, H., AND YOSHIDA, K. Monosynaptic activation of medium-lead burst neurons from the superior colliculus in the alert cat. *J. Neurophysiol.* 75: 2658–2661, 1996.

DROULEZ, J. AND BERTHOZ, A. Spatial and temporal transformations in visuo-motor coordination. In: *Neural Computers,* edited by R. Eckmiller and C. von der Malsburg. Berlin: Springer-Verlag, 1988, p. 345–357.

ERKELENS, C. J. AND SLOOT, O. B. Initial direction and landing positions of binocular saccades. *Vision Res.* 35: 3297–3303, 1995.

ERKELENS, C. J. AND VOGELS, I.M.L.C. The relationship between the initial direction and landing position of saccades. In: *Eye Movements Research: Mechanisms, Processes and Applications,* edited by J. Findlay, J. R. Walker and R. W. Kentridge. Amsterdam: Elsevier, 1995, p. 133–144.

EVINGER, C. AND FUCHS, A. F. Saccadic, smooth pursuit and optokinetic eye movements of the trained cat. *J. Physiol. (Lond.)* 285: 209–229, 1978.

EVINGER, C., KANEKO, C.R.S., AND FUCHS, A. F. Oblique saccadic eye movements of the cat. *Exp. Brain Res.* 41: 370–379, 1981.

FUCHS, A. F., ROBINSON, F. R., AND STRAUBE, A. Role of the caudal fastigial nucleus in saccade generation. I. Neuronal discharge patterns. *J. Neurophysiol.* 70: 1723–1740, 1993.

GROSSMAN, G. E. AND ROBINSON, D. A. Ambivalence in modelling oblique saccades. *Biol. Cybern.* 58: 13–18, 1988.

GUITTON, D. AND MANDL, G. Oblique saccades of the cat: a comparison between the durations of horizontal and vertical components. *Vision Res.* 20: 875–881, 1980.

HEPP, K., HENN, V., VILIS, T., AND COHEN, B. Brainstem regions related to saccade generation. In: *The Neurobiology of Saccadic Eye Movements, Reviews of Oculomotor Research,* edited by R. H. Wurtz and M. E. Goldberg. Amsterdam: Elsevier, 1989, vol. 3, p. 105–212.

HIKOSAKA, O. AND WURTZ, R. H. Modification of saccadic eye movements by GABA-related substances. I. Effect of muscimol and bicuculline in monkey superior colliculus. *J. Neurophysiol.* 53: 266–291, 1985.

JÜRGENS, R., BECKER, W., AND KORNHUBER, H. H. Natural and drug-induced variations of velocity and duration of human saccadic eye movements: evidence for a control of the neural pulse generator by local feedback. *Biol. Cybern.* 39: 87–96, 1981.

KANEKO, C.R.S., EVINGER, C., AND FUCHS, A. F. Role of cat pontine burst neurons in generation of saccadic eye movements. *J. Neurophysiol.* 46: 387–408, 1981.

KELLER, E. L. AND ROBINSON, D. A. Abducens unit behavior in the monkey during vergence movements. *Vision Res.* 12: 369–382, 1972.

KING, W. M. AND FUCHS, A. F. Reticular control of vertical saccadic eye movements by mesencephalic burst neurons. *J. Neurophysiol.* 42: 861–876, 1979.

KING, W. M., LISBERGER, S. G., AND FUCHS, A. F. Oblique saccadic eye movements of primates. *J. Neurophysiol.* 56: 769–784, 1986.

LEFÈVRE, P. AND GALIANA, H. L. Dynamic feedback to the superior colliculus in a neural network model of the gaze control system. *Neural Networks.* 5: 871–890, 1992.

MOSCHOVAKIS, A. K. AND HIGHSTEIN, S. M. The anatomy and physiology of primate neurons that control rapied eye movements. *Annu. Rev. Neurosci.* 17: 465–488, 1994.

MOSCHOVAKIS, A. K., SCUDDER, C. A., AND HIGHSTEIN, S. M. Structure of the primate burst generator. I. Medium-lead burst neurons with upward on-directions. *J. Neurophysiol.* 65: 203–217, 1991a.

MOSCHOVAKIS, A. K., SCUDDER, C. A., HIGHSTEIN, S. M., AND WARREN, J. D. Structure of the primate burst generator. II. Medium-lead burst neurons with downward on-directions. *J. Neurophysiol.* 65: 218–229, 1991b.

MUNOZ, D. P. AND WURTZ, R. H. Saccade-related activity in monkey superior colliculus. II. Spread of activity during saccades. *J. Neurophysiol.* 73: 2334–2348, 1995.

NICHOLS, M. J. AND SPARKS, D. L. Component stretching during oblique stimulation-evoked saccades: the role of the superior colliculus. *J. Neurophysiol.* 76: 582–600, 1996.

OPTICAN, L. M. Control of saccade trajectory by the superior colliculus. In: *Contemporary Ocular Motor and Vestibular Research: A Tribute to David A. Robinson,* edited by A. F. Fuchs, T. Brandt, U. Büttner, and D. S. Zee. Stuttgart: Thieme, 1994, p. 98–105.

OPTICAN, L. M. A field theory of saccade generation: temporal-to-spatial transform in the superior colliculus. *Vision Res.* 35: 3313–3320, 1995.

OPTICAN, L. M., QUAIA, C., AND LEFÈVRE, P. A new model of the saccadic system: I. Separate modules for specifying direction and duration. *Soc. Neurosci. Abstr.* 22: 1457, 1996.

OPTICAN, L. M. AND ROBINSON, D. A. Cerebellar-dependent adaptive control of primate saccadic system. *J. Neurophysiol.* 44: 1058–1076, 1980.

OTTES, F. P., VAN GISBERGEN, J.A.M., AND EGGERMONT, J. J. Visuomotor fields of the superior colliculus: a quantitative model. *Vision Res.* 26: 857–873, 1986.

QUAIA, C. AND OPTICAN, L. M. Neural decomposition of oblique eye movements into horizontal and vertical components. *Soc. Neural Control Movement Abstr.* 1: 25, 1996.

ROBINSON, D. A. A method of measuring eye movement using a scleral search coil in a magnetic field. *IEEE Trans. Bio-Med. Eng.* 10: 137–145, 1963.

ROBINSON, D. A. Eye movements evoked by collicular stimulation in the alert monkey. *Vis. Res.* 12: 1795–1808, 1972.

ROBINSON, D. A. Models of the saccadic eye movement control system. *Kybernetik.* 14: 71–83, 1973.

ROBINSON, D. A. Oculomotor control signals. In: Basic *Mechanisms of Ocular Motility and Their Clinical Implications,* edited by G. Lennerstrand and P. Bach-y-Rita. Oxford: Pergamon Press, 1975, p. 337–374.

ROBINSON, D. A. The use of matrices in analyzing the three-dimensional behavior of the vestibulo-ocular reflex. *Biol. Cybern.* 46: 53–66, 1982.

SCHILLER, P. H. AND KOERNER, F. Discharge characteristics of single units in superior colliculus of the alert rhesus monkey. *J. Neurophysiol.* 34: 920–936, 1971.

SCHILLER, P. H. AND STRYKER, M. Single-unit recording and stimulation in superior colliculus of the alert rhesus monkey. *J. Neurophysiol.* 35: 915–924, 1972.

SCUDDER, C. A., FUCHS, A. F., AND LANGER, T. P. Characteristics and functional identification of saccadic inhibitory burst neurons in the alert monkey. *J. Neurophysiol.* 59: 1430–1454, 1988.

SMIT, A. C., VAN OPSTAL, A. J., AND VAN GISBERGEN, J.A.M. Component stretching in fast and slow oblique saccades in the human. *Exp. Brain Res.* 81: 325–334, 1990.

SPARKS, D. L. AND MAYS, L. E. Signal transformations required for the generation of saccadic eye movements. *Annu. Rev. Neurosci.* 13: 309–336, 1990.

SPARKS, D. L., MAYS, L. E., AND PORTER, J. D. Eye movements induced by pontine stimulation: interaction with visually triggered saccades. *J. Neurophysiol.* 58: 300–317, 1987.

STRASSMAN, A., HIGHSTEIN, S. M., AND MCCREA, R. A. Anatomy and physiology of saccadic burst neurons in the alert squirrel monkey. I. Excitatory burst neurons. *J. Comp. Neurol.* 249: 337–357, 1986a.

STRASSMAN, A., HIGHSTEIN, S. M., AND MCCREA, R. A. Anatomy and physiology of saccadic burst neurons in the alert squirrel monkey. II. Inhibitory burst neurons. *J. Comp. Neurol.* 249: 358–380, 1986b.

TWEED, D. B. AND VILIS, T. A two dimensional model for saccade generation. *Biol. Cybernetics.* 52: 219–227, 1985.

VAN GISBERGEN, J.A.M., ROBINSON, D. A., AND GIELEN, S. A quantitative analysis of generation of saccadic eye movements for burst neurons. *J. Neurophysiol.* 45: 417–442, 1981.

VAN GISBERGEN, J.A.M., VAN OPSTAL, A. J., AND SCHOENMAKERS, J.J.M. Experimental test of two models for the generation of oblique saccades. *Exp. Brain Res.* 57: 321–336, 1985.

VAN OPSTAL, A. J. AND KAPPEN, H. A two-dimensional ensemble coding model for spatial-temporal transformation of saccades in monkey superior colliculus. *Network* 4: 19–38, 1993.

VIVIANI, P., BERTHOZ, A., AND TRACEY, D. The curvature of oblique saccades. *Vision Res.* 17: 661–664, 1977.

WAITZMAN, D. M., MA, T. P., OPTICAN, L. M., AND WURTZ, R. H. Superior colliculus neurons mediate the dynamic characteristics of saccades. *J. Neurophysiol.* 66: 1716–1737, 1991.

WURTZ, R. H. AND GOLDBERG, M. E. Superior colliculus responses related to eye movement in awake monkeys. *Science* 171: 82–84, 1971.

WURTZ, R. H. AND GOLDBERG, M. E. Activity of superior colliculus in behaving monkey. III. Cells discharging before eye movements. *J. Neurophysiol.* 35: 575–586, 1972.

ZEE, D. S., OPTICAN, L. M., COOK, J. D., ROBINSON, D. A., AND ENGEL, W. K. Slow saccades in spinocerebellar degeneration. *Arch. Neurol.* 33: 243–251, 1976.